CHAPTER 2

RESULTS AND DISCUSSION

2.1 Synthesis of (+)-Castanospermine (1a)

In order to develop an efficient approach for synthesizing our target, polyhydroxylated indolizidines and polyhydroxylated pyrrolizidines, castanospermine **1a** was the first molecule to be derived from our synthetic route. Due to the same stereochemistry at C-6, C-7 and C-8 of castanospermine **1a** as L-xylose **177**, this was used as the starting molecule. The *S*-hydroxy functionality at C-1 in **1a** was formed from ring opening of the cyclic sulfate-oxazolidinone which was derived from the corresponding pyrrolo[1,2-*c*]oxazol-3-ones.

2.1.1 Synthesis of Pyrrolo[1,2-*c*]oxazol-3-ones

2.1.1.1 Petasis Reaction

Pyrrolo[1,2-*c*]oxazol-3-ones are one of our important building blocks for conversion into polyhydroxylated pyrrolizidines and polyhydroxylated indolizidines such as, castanospermine (**1a**), swainsonine (**3**) [104] and epimers of austaline [107]. They can be obtained by derivatisation reactions starting with the Petasis reaction (boronic acid-Mannich reaction) [269] to condense three components, L-xylose, *trans*-2-phenylboronic acid and allylamine into the optically pure *β*-amino alcohol diene **176** (Scheme 22). The yield of the desired products was 90% after purification by ion-exchange chromatography. The ^{1}H and ^{13}C NMR spectral data of this compound matched those reported in the literature [132]. The exact mechanism of the borono-

Mannich reaction is not known, we speculate that these reactions occur via the boronate complex intermediate **A** (Figure 14), in which the iminium ion adopts the reactive conformation shown to minimize 1,3-allylic strain [103]. A possible reaction mechanism to form intermediate **A** is nucleophilic addition of the amino group in allylamine **179** to the aldehyde carbonyl of L-xylose **177** to give an iminium ion. The boronic acid then formed the corresponding boronate **A** via coordination with the C-2 hydroxy of the L-xylose. The coordination of boron to the hydroxyl group at the other positions is also possible and these coordination processes would be reversible. However, such intermediates would be expected to give Petasis products at a much slower rate than intermediate **A**.

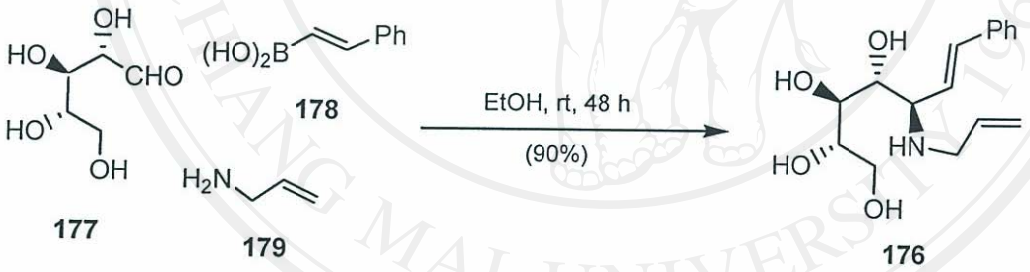

Scheme 22

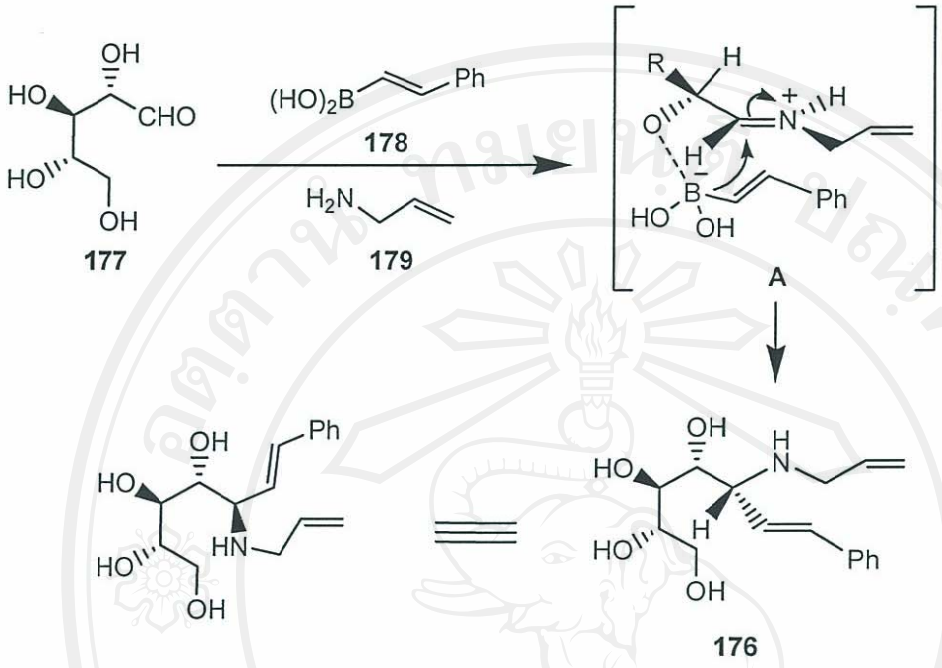

Figure 14 Possible mechanism of the formation of β-amino alcohol diene **176** via the boronate complex intermediate **A**.

2.1.1.2 Synthesis of Oxazolidinones

To protect both of the amino group and the C-4 hydroxyl groups in **176** this compound was treated with triphosgene (0.33 eq.) in the presence of triethylamine in THF to give a mixture of the oxazolidinones **180** and **181**. These compounds were readily separated by column chromatography in yields of 53% and 5.4%, respectively. Unsuccessful reagents and conditions to generate the oxazolidinones were shown in Table 5. The CO signal at 159.8 ppm for **180** in the ^{13}C-NMR spectrum indicated the formation of desired oxazolidione **180**, and the two CO signals at 159.9 and 162.1 ppm showed the formation of dioxolanoyl oxazolidinone **181**. Oxazolidinone **180** was also recovered from dioxolanoyl oxazolidinone **181** by hydrolysis with K_2CO_3 in

methanol at room temperature for 3 days, in 96% yield (Scheme 23). We believe the oxazolidinone **181** occurred from the reaction of triphosgene with the free primary and secondary adjacent hydroxyl groups of **176** or **180** (Figure15).

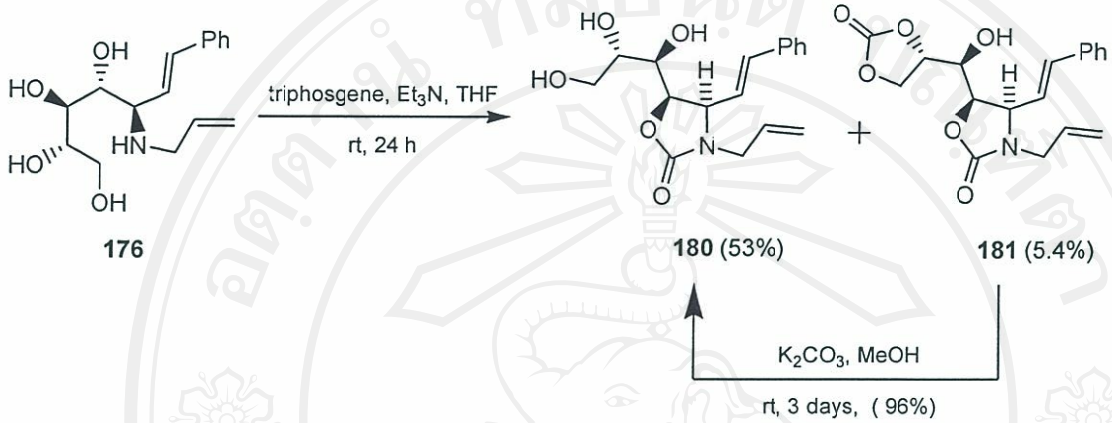

Scheme 23

Table 5 Reagents and results of attempted oxazolidinones formation

Entry	Reagents	Result*
1	Triphosgene, Et_3N, CH_3CN, DMF, 0 °C to rt, 24 h	NR
2	Triphosgene, Et_3N, DCM (dry), 0 °C to rt, 24 h	NR

* NR = No Reaction

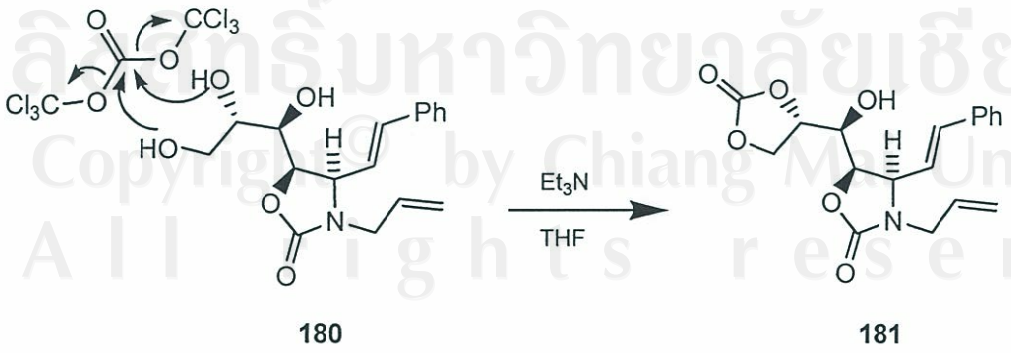

Figure 15 Reaction mechanism of triphosgene and oxazolidinone **180** to form dioxalanoyl oxazolidinone **181**

2.1.1.3 Protection of the Hydroxyl Groups

The three hydroxyl groups of oxazolidinone **180** were sequentially protected. The primary hydroxy group was first protected by treatment with trityl chloride (1.5 eq.) in pyridine solution. After separation by column chromatography, the trityl ether **182** was obtained in 87% yield. The ^{1}H-NMR spectrum of **182** showed signals at 7.39-7.19 ppm (20 aromatic H; 15H from trityloxy group and 5H from phenylvinyl group) and 3.18 and 3.31 ppm (2H of H-3'). The chemical shift values of H-3' in the trityl ether **182** moved to higher field by the inductive effect of the trityloxy group that was connected to C-3'. The resulting trityl ether **182** was di-*O*-benzylated by treatment with NaH (2.5 eq.), benzyl bromide (8 eq.) and a catalytic amount tetrabutylammonium iodide in dry THF solution to afforded a mixture of the bisbenzylated oxazolidinone **183** in 56% yield and the undesired product bisbenzylated oxazinanone **184** in a yield of 22% after separation by column chromatography (Scheme 24).

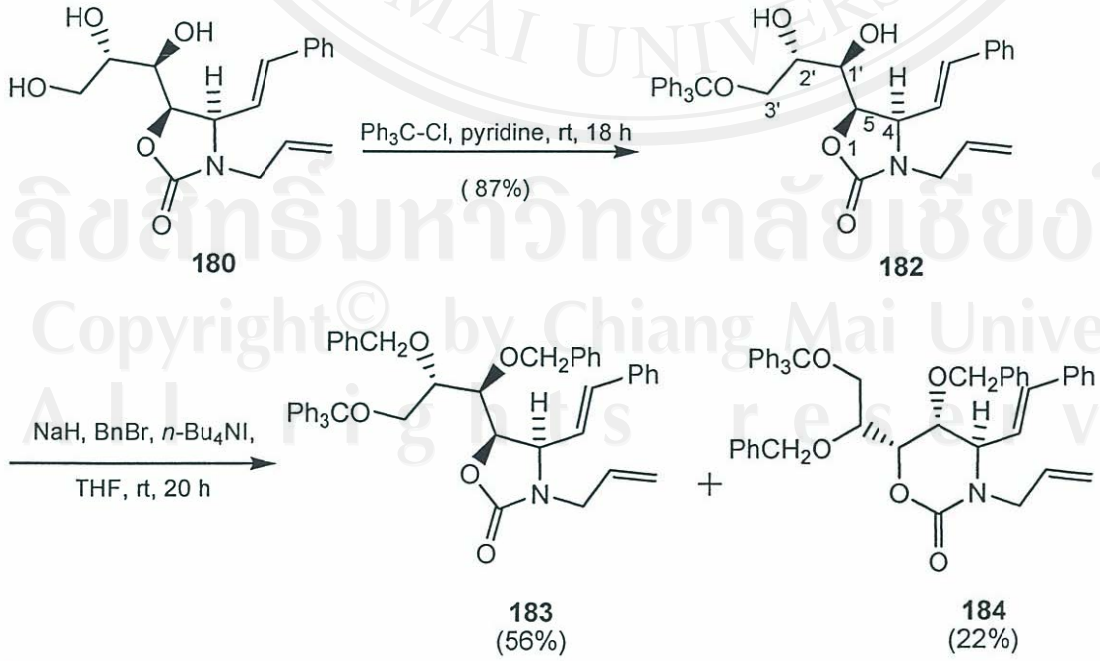

Scheme 24

A mechanism for formation of the undesired oxazinanone **184** is shown in Scheme 25. The C-1' hydroxyl is deprotonated by NaH and the corresponding C-1' alkoxide can add to the carbonyl of the oxazolidinone to expand the ring from a five membered ring to a six membered ring of the oxazinanone **184**.

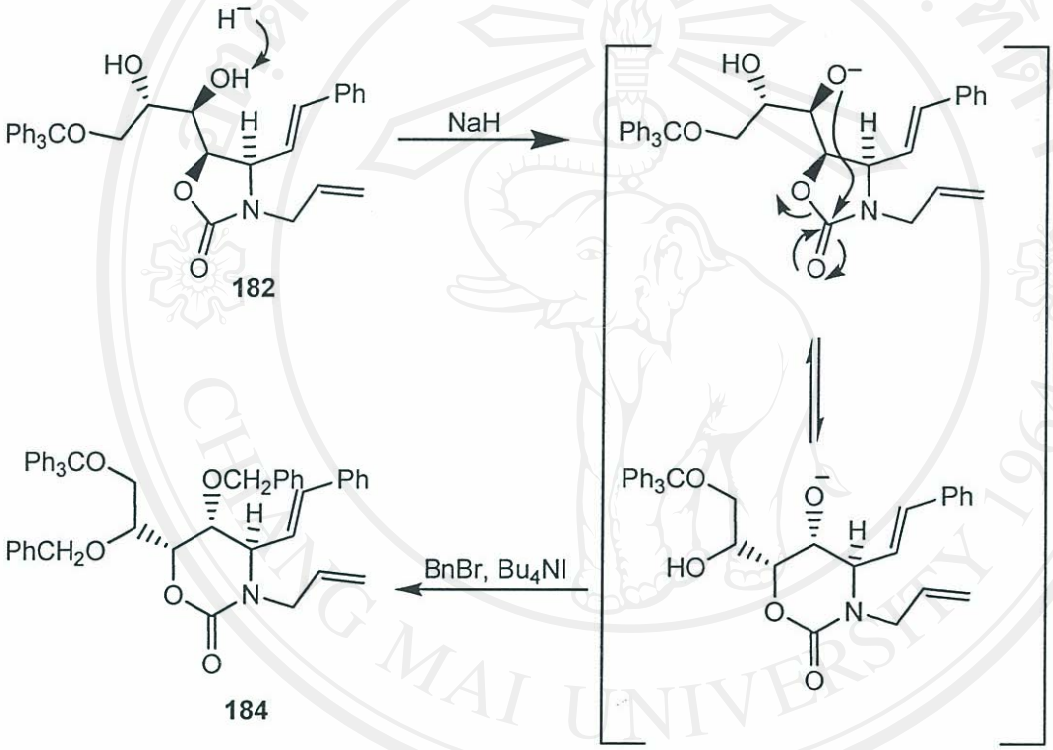

Scheme 25 Possible mechanism of generation of the oxazinanone **184**

The ^{13}C NMR spectra of **183** and **184** showed CO resonances at 162.2 and 152.1 ppm, respectively, consistant with their respective 5- and 6-membered ring structures. The chemical shifts for CH-5 and CH-1' of the oxazolidinone **183** and for CH-5 and CH-6 of oxazinanone **184** are shown in Figure 16.

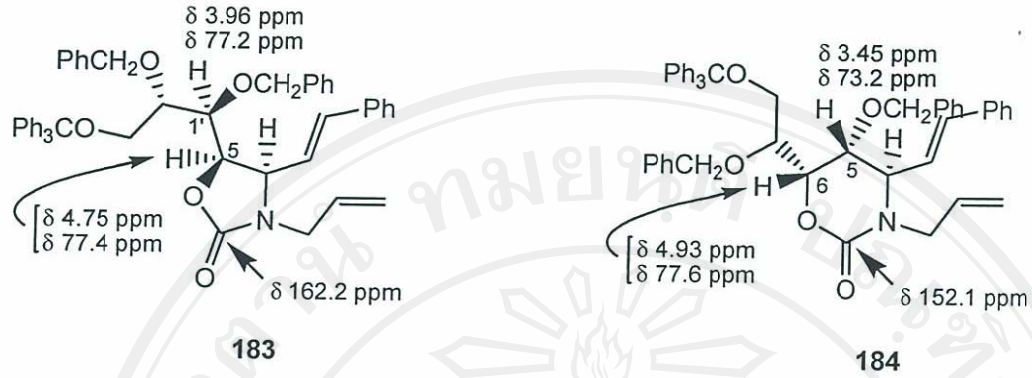

Figure 16 Chemical shifts of CH-5 and CH-1' in oxazolidinone **183** and CH-5 and CH-6 in oxazinanone **184**

Further evidence for the structures of **183** and **184** was the downfield shift in the ^{1}H NMR spectrum of CH-5 and CH-6 in these compounds, respectively.

Due to the similar mobilities of **183** and **184** on silica gel (Rf_{183} = 0.60 and Rf_{184} = 0.55 in 40% EtOAc/petrol) they were hard to separate. Fortunately the mixture could be used in the next step of ring-closing metathesis (RCM) without separation.

2.1.1.4 Ring-Closing Metathesis (RCM)

RCM is one of the key steps in our proposed approach. In 1995, Blechert and Huwe revealed that the RCM reaction of the simple oxazolidinone **185** with Grubbs' I catalyst (benzylidine bis(tricyclohexylphosphine)dichlororuthenium) in benzene at rt did not occur [270]. However, Nicole Gates, who worked in Pyne's laboratory, showed that the RCM reaction of **185** and **186** were relatively slow but worked efficiently when heating a dilute DCM solution of the oxazolidinone **185** or **186** with Grubb's II catalyst (**148**) at reflux (Scheme 26) [106]. With the mixture of hindered

oxazolidinone diene **183** and oxazinanone diene **184** in hand, the RCM reaction was expected to require the reaction conditions developed by Gates. Therefore, heating a 3.5 : 1 mixture of **183** and **184** with Grubbs' II catalyst (7 mol%) at reflux in a highly diluted DCM solution for 24 h resulted in the formation of the separable pyrrolo[1,2-*c*]oxazol-3-one **189** and pyrrolo[1,2-*c*][1,3]oxazin-1-one **190** in the yield of 68% and 20%, respectively. (Scheme 27). The success of the RCM on the oxazolidinone diene **183** and the oxazinanone diene **184** was indicated by changes from six alkene protons in the starting materials to two in the products in the ^{1}H NMR spectrum and disappearance of two alkene CH_2 signals in the ^{13}C NMR spectrum.

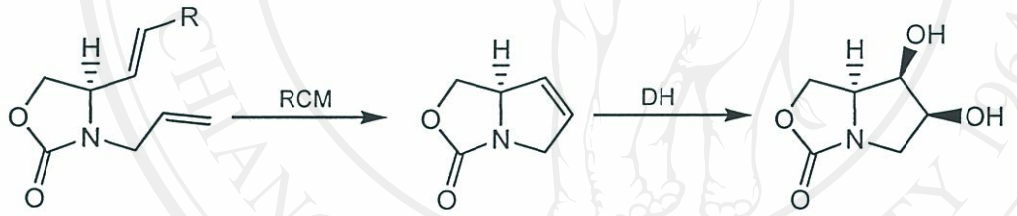

185 R = H
186 R = Ph

187

188

Scheme 26 RCM of simple oxazolidinones **185** and **186**

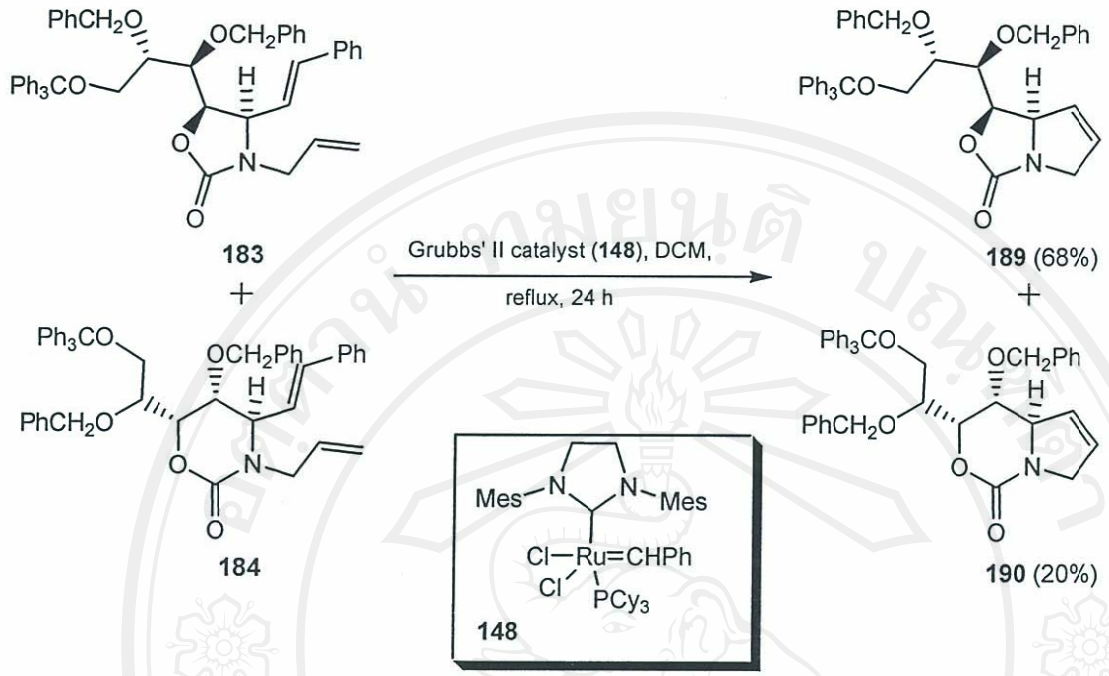

Scheme 27

2.1.2 Synthesis of 7*S*-Hydroxy-pyrrolo[1,2-*c*]oxazol-3-one (194)

2.1.2.1 Syn-Dihydroxylation

Due to the (*S*)-C-1 hydroxy functionality in castanospermine **1a**, our plan considered a sequence by formation of an epoxide from the alkene **189** and then selective ring opening with hydride to give the desired alcohol **194**. However, reaction of **189** with either dimethyl dioxirane or with *m*-CPBA was unsuccessful. The reagents and results of the epoxidation of **189** are summarized in Table 6.

Scheme 28

Table 6 Reagents and results of epoxidation of the alkene **189**

Entry	Reagents	Results
1	*m*-CPBA, DCM	Starting Material
2	Dimethyl dioxirane, acetone	Complex Mixture

In our first attempt we treated **189** with *m*-CPBA in DCM solution. This reaction resulted in recovered unreacted starting material. The last attempt was not effective either, treatment of the alkene **189** with dimethyl dioxirane, that was generated in situ from the reaction of acetone and oxone™, resulted in a complex mixture of products.

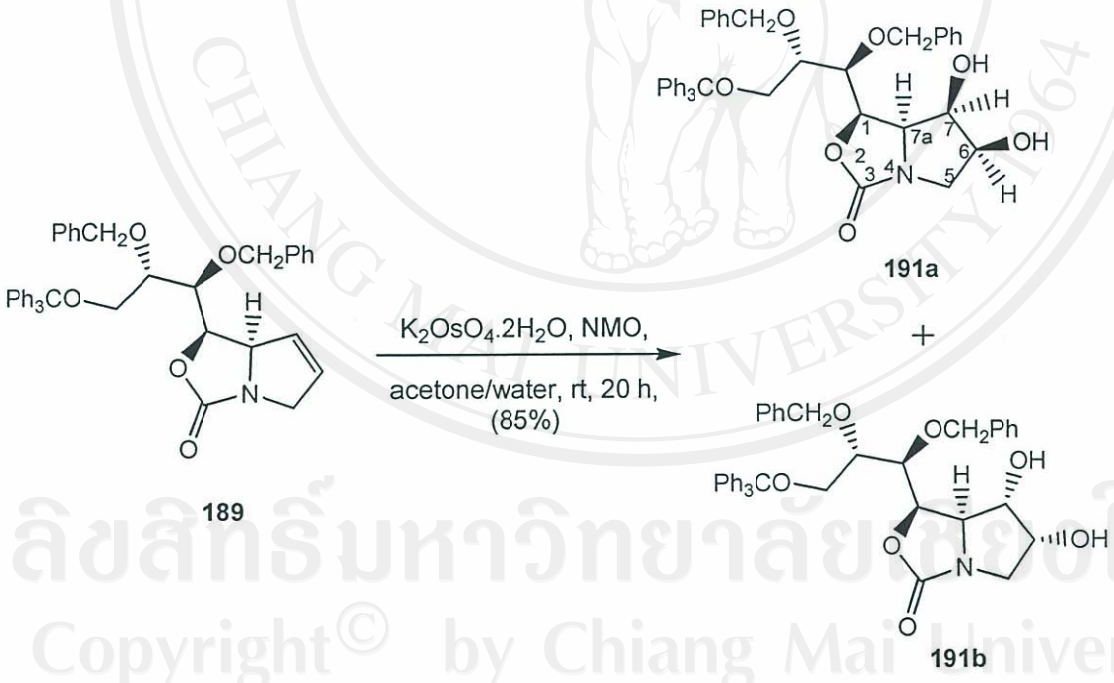

Scheme 29

Consequently, in an alternative approach, *syn*-dihydroxylation (DH) of the double bond of **189** employing $K_2OsO_4.2H_2O$ (6 mol%) and NMO as co-oxidant [271] in a mixture of acetone and H_2O at rt for 20 h was attempted (Scheme 29). We found that the *syn*-dihydroxylation of **189** gave a 83:17 mixture of the diastereoisomers, **191a** and **191b**, in favor of the diastereomer **191a**, having the absolute stereochemistry at C-7 the same as that of C-1 of castanospermine **1a**. The stereochemical outcomes of this DH reaction was expected due to the more stereodirecting effect of the pseudo-axial allylic protons H5α and H7a on the α-face of **189**. Figure 17 shows a molecular model (PC Spartan Pro AM1) of **189** and the preferred direction attack of the osmium reagent to the least hinder of β-face (convex face) of the alkene **189**. This approach is less favored by the C-1 substituent which may account for the reduced diastereoselectivity of the DH reaction in comparison with the DH of **187** which gave **188** with 100% diastereoselection (Scheme 26) [106].

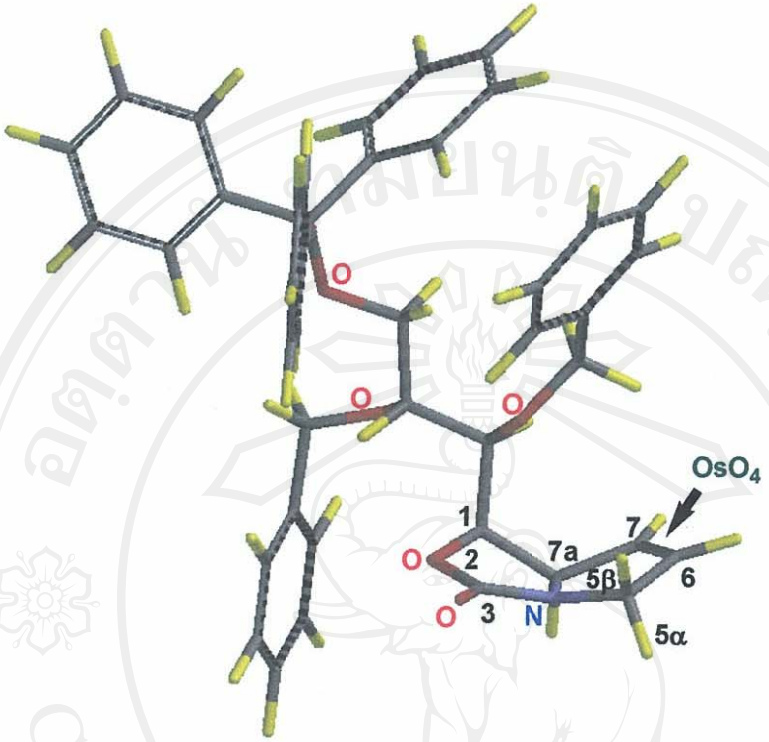

Figure 17 Molecular Model (PC Spartan Pro AM1) of **189**

The resulting isomers could be separated employing 2% MeOH/DCM as an eluent on a silica gel column. The success of the DH was indicated by the disappearance of the alkene signals at 5.65 ppm and 5.84 ppm in the ^{1}H NMR spectrum and the loss of two alkene CH signals at 126.2 ppm and 131.7 ppm in the ^{13}C NMR spectrum. The stereochemistry was evident from NOESY studies on the diol **191a** that showed significant cross peaks between H-6 and H-7, between H-7 and H-7a and H-7a and H-6. (see Scheme 29 for proton numbering and Figure 18 for the NOESY relationship of the diol **191a**).

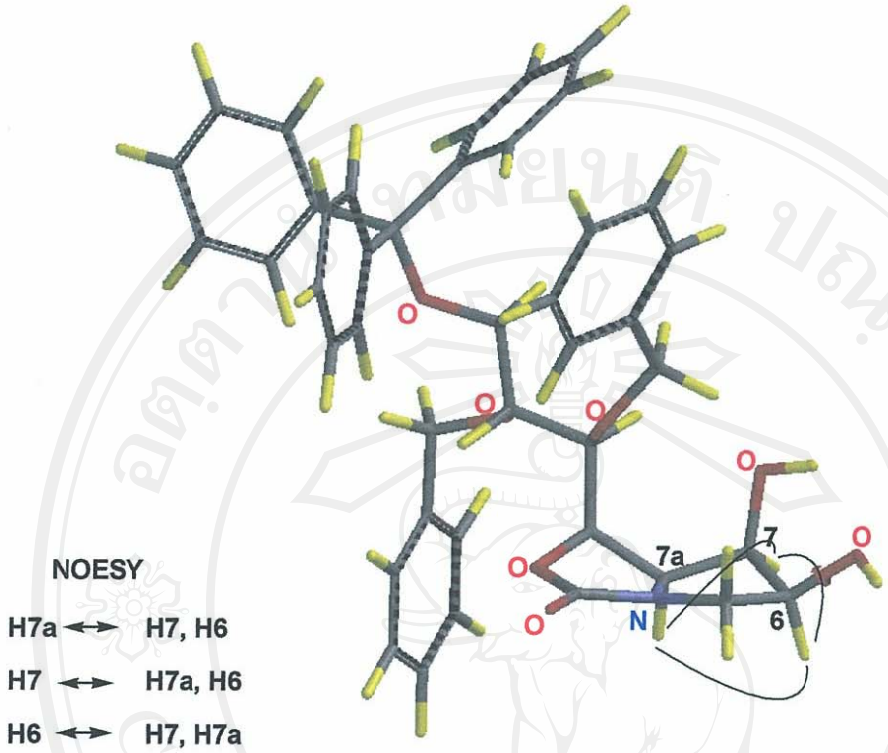

Figure 18 Molecular Model (PC Spartan Pro AM1) of **191a** and NOESY correlation of H-6, H-7 and H7a)

2.1.2.2 Synthesis of the Cyclic-sulfate and the Ring Opening

The diol **191a** was converted to its cyclic-sulfate **193** [260, 261] using thionyl chloride to first give the cylic-sulfite **192**, followed by oxidation with catalytic ruthenium tetroxide/stoichiometric $NaIO_4$ (64% yield for the two-step conversion) (Scheme 30). Owing to the effect from the cyclic sulfate ring, H-3a and H-8a of **193** moved further downfield in the ^{1}H-NMR spectrum from 3.54 ppm to 4.80 ppm (H-3a) and from 4.14 ppm to 5.05 ppm (H-8a). Consistently, C-3a also moved downfield from 70.8 ppm to 83.6 ppm and C-8a from 74.1 ppm to 84.3 ppm in the ^{13}C-NMR spectrum of **193**.

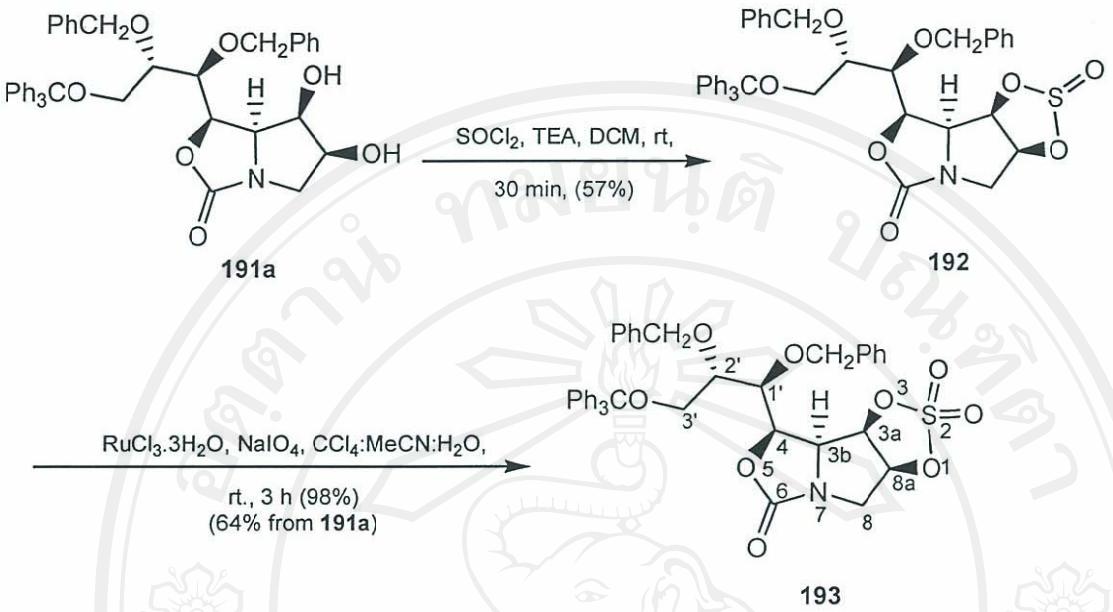

Scheme 30

Regioselective nucleophilic ring opening of the dioxo-dioxathiole ring of **193** with $NaBH_4$, followed by an acid-catalysed hydrolysis of the intermediate acyclic sulfate gave the diol **194** in 63% yield (Scheme 31). Nucleophillic attack on **193** would be expected to occur preferentially at the least hindered C-8a position since backside attack at C-3a would be more sterically demanding due to the β-C-1 bis(benzyloxy)-triphenylmethoxypropyl substituent (Figure 19). Because of the acid sensitivity of the trityl ether moiety, the final product was detritylated during the acid hydrolysis step. The appearances of 2 H-6 signals at 1.74 and 1.93 ppm in the ^{1}H spectrum and the C-6 signal at 34.5 ppm in the ^{13}C NMR spectrum indicated the successful cleavage of the cyclic sulfate ring. The loss of 15 aromatic protons in the ^{1}H-NMR spectrum of **194** clearly indicated that detritylation had occured.

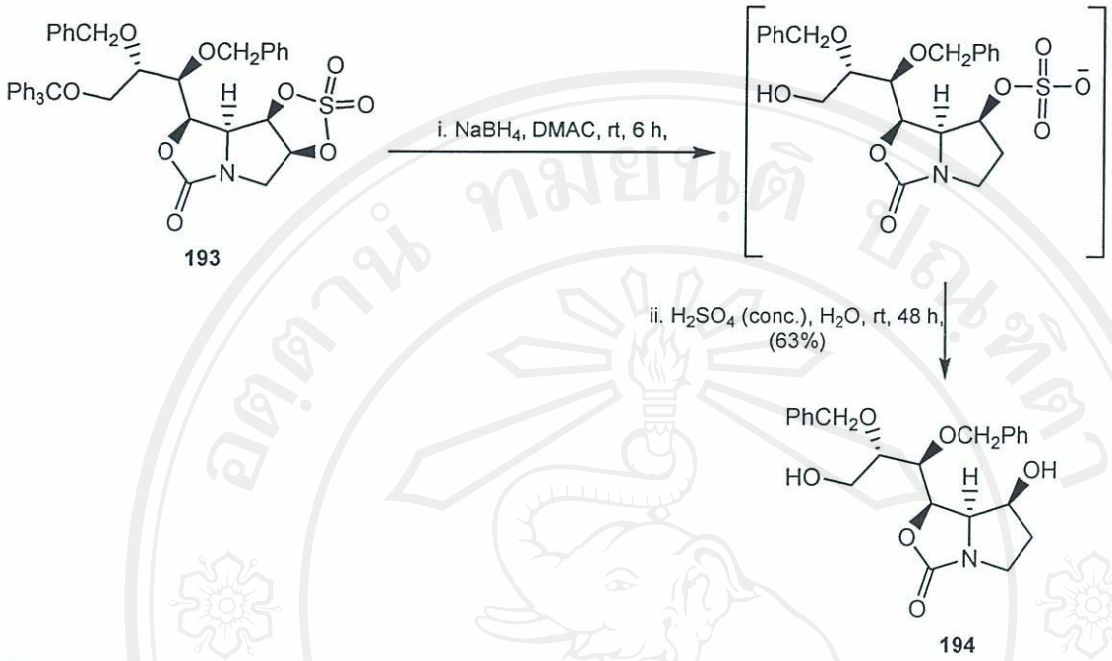

Scheme 31

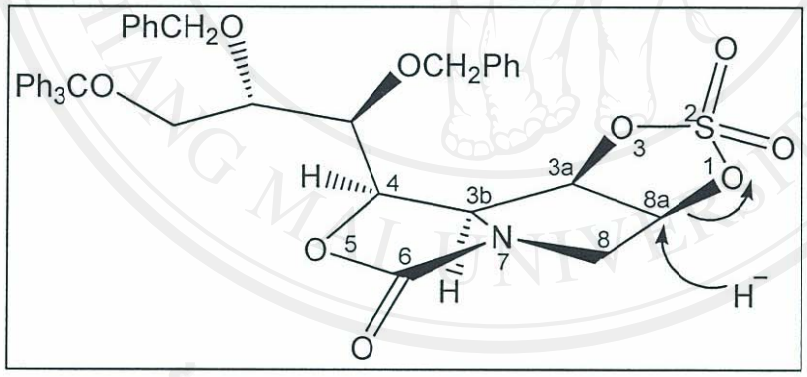

Figure 19 Mechanism of cyclic-sulfate ring opening by the hydride ion from $NaBH_4$. Nucleophilic attack at the less hindered C-8a position of **193**.

2.1.2.3 Deprotection of the Oxazolidinone Ring of 194

Base hydrolysis of the oxazolidinone ring of **194** was performed by treatment with NaOH in MeOH solution. The reaction mixture was heated in a microwave

reactor at 110 °C for 2 h and gave the desired amino triol **195** in a yield of 80% and the side product **196** (16% yield) (Scheme 32).

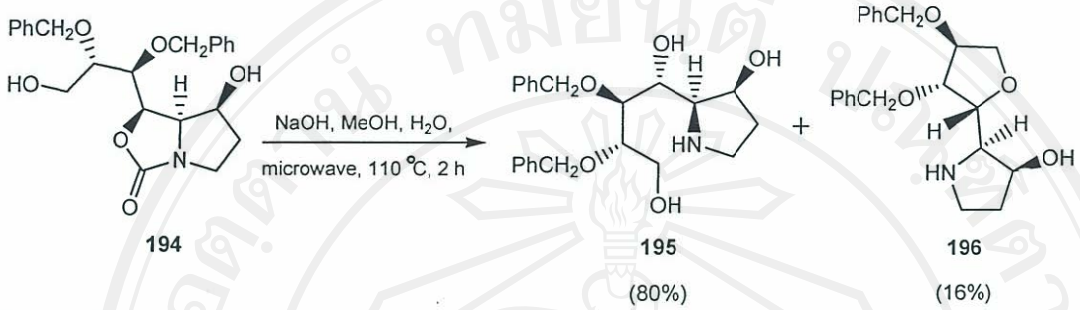

Scheme 32

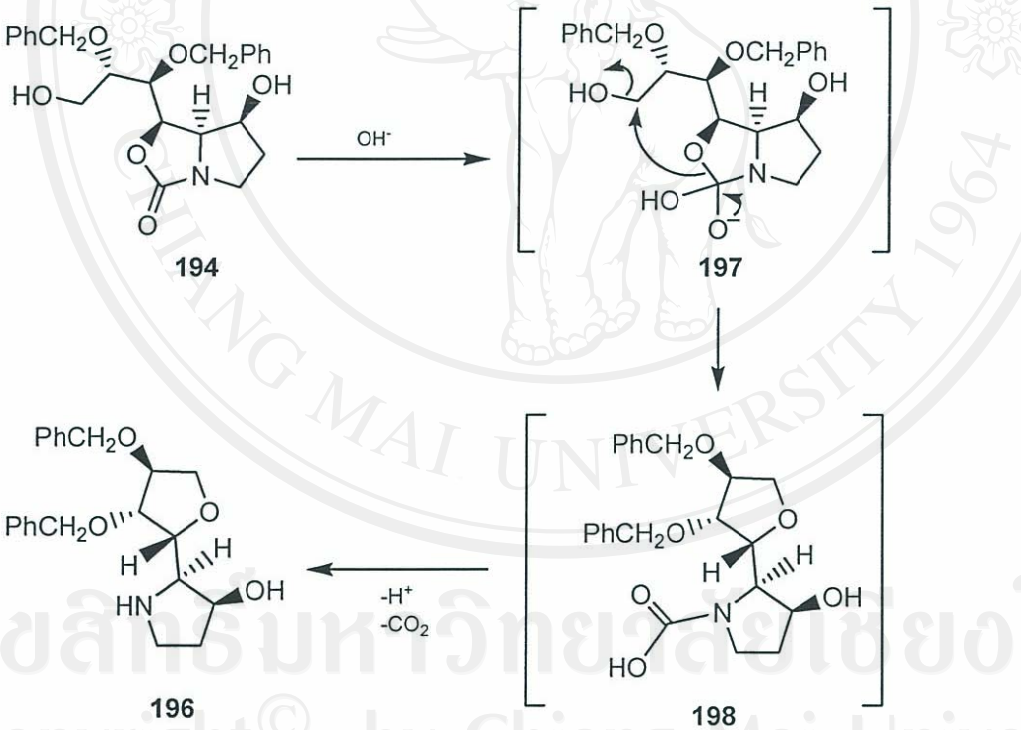

Figure 20 The possibility pathway to generate the side product **196** by the base hydrolysis under microwave heating.

The formation of **196** was unexpected due to the addition of hydroxide ion to the carbonyl carbon of the oxazolidinone ring of **194** to form the intermediate **197**. The intermediate **198** was then occurred by the driving force from the negative charge on the oxygen atom of the compound **197**. Deprotonation and decarboxylation of compound **198** afforded the side product **196** (Figure 20). Disappearance of the CO group signal of the oxazolidinone ring and the downfield shift of the C-1' signal of **195** at 78.9 ppm (possibly inductive effect from the benzyloxy group at C-2') in the ^{13}C NMR spectrum and the highfield shift of the H-1' signal of **195** at 4.81 ppm in the ^{1}H-NMR spectrum indicated the successful cleavage of the oxazolidinone ring. The downfield shift of the C-5' signal of **196** at 72.0 ppm in the ^{13}C NMR spectrum indicated this carbon connected to the oxygen atom and the downfield shift of the 2 H-5' signals of **196** at 3.90 and 4.02 ppm in ^{1}H-NMR spectrum indicated the formation of the tetrahydrofuranyl pyrrolidine **196**. The MS spectrum of **196** indicated loss of H_2O from **195**.

2.1.3 Mitsunobu Cyclization

With further investigation on the cyclization of amino alcohol **195**, the Mitsunobu reagent was found popular and useful in forming azetidines [271-273], pyrrolidines [274-278], piperidines [279] and indolizidines [280].

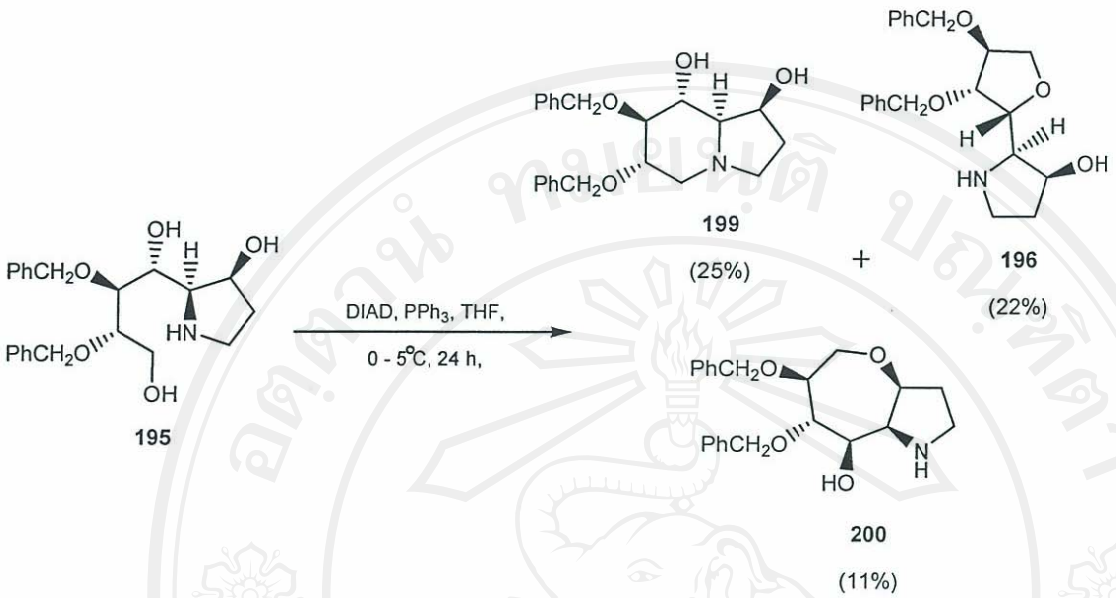

Scheme 33

A mixture of PPh_3 and diethyl azodicaboxylate (DEAD) is generally used in the Mitsunobu reaction; however, diisopropyl azodicaboxylate (DIAD) is cheaper and less toxic and works just as well. With DIAD in hand, the Mitsunobu reaction was conducted by treatment of the amino alcohol **195** with PPh_3 and DIAD in dry THF at 0 °C to 5 °C for 24 h. This reaction gave the target indolizidine **199** in a low yield (25 %) and the two side products **196** and **200** in yields of 22% and 11%, respectively (Scheme 33). The mechanism of the Mitsunobu cyclization reaction of **195** [277] is outlined in Scheme 33, 34 and 35. As in the Appel cyclization an oxy-phosphonium intermediate **201** is formed which undergoes cyclization to **199** (Scheme 34), **196** or **200** (Scheme 35).

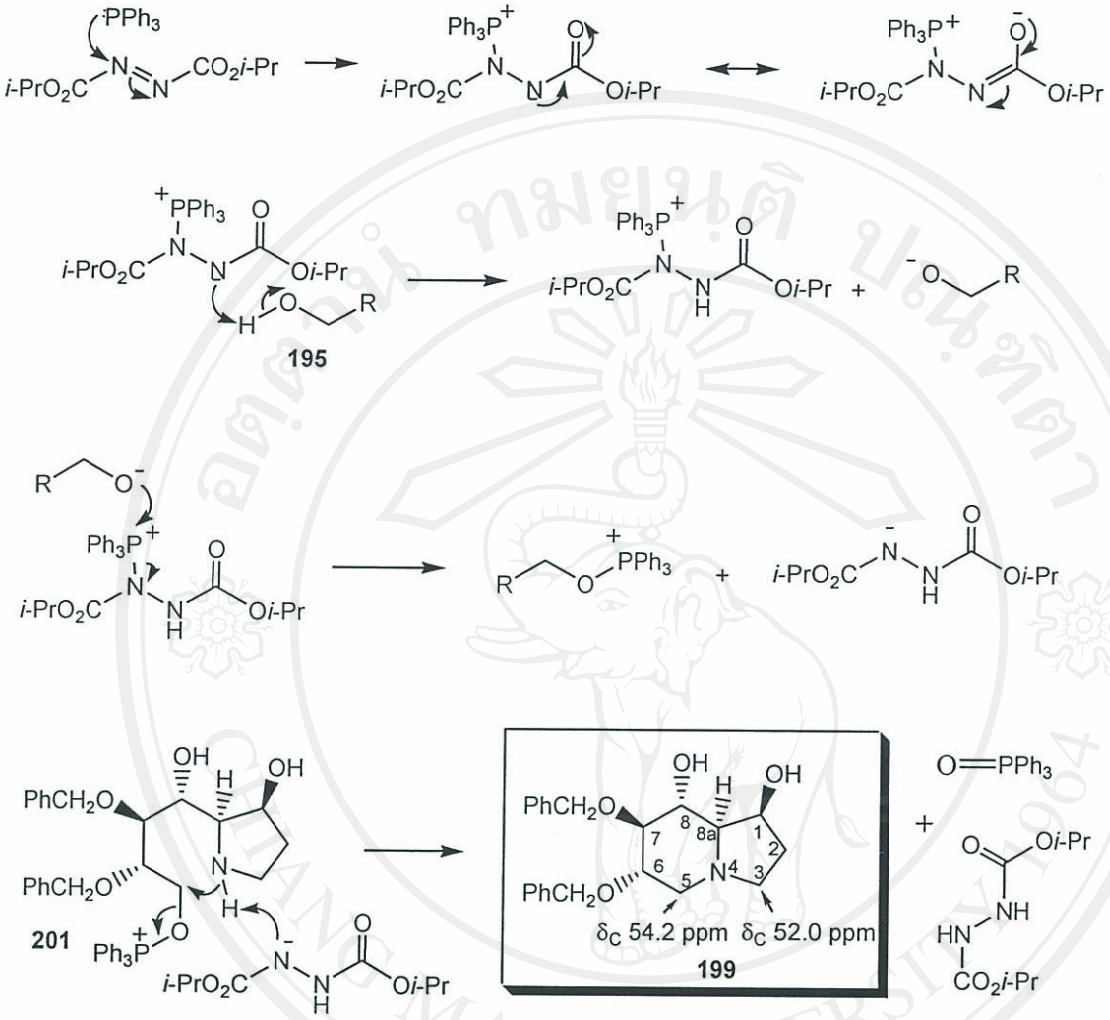

Scheme 34 Mechanism of the Mitsunobu reaction.

The pyrrolidine side product **196**, which was identical to that obtained from the hydrolysis of **194**, was obtained by bond formation between the oxygen atom of the hydroxy at C-1' and phosphonuim oxide carbon (Figure 35 A) while compound **200** was obtained by bond formation between the oxygen atom of the hydroxy at C-3 and phosphonuim oxide carbon of the intermediate **201**, (Scheme 35).

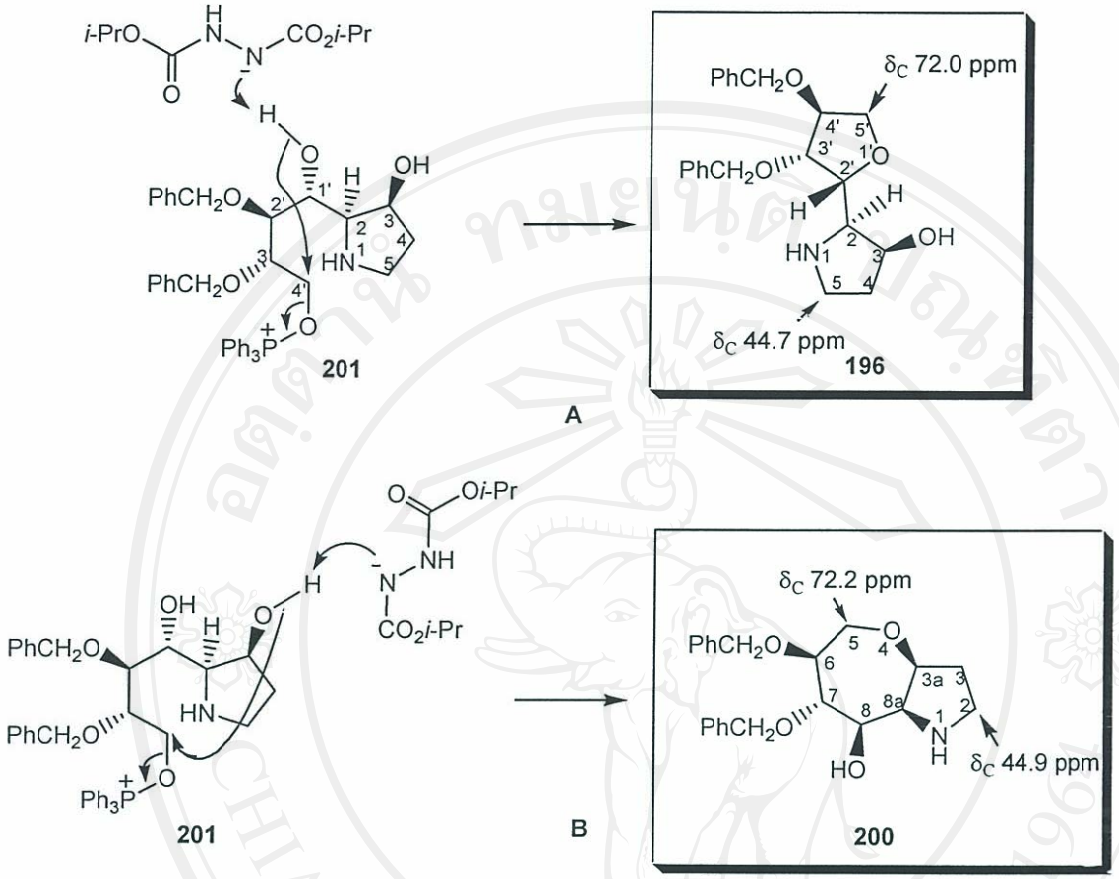

Scheme 35 Formations of the side products, **196** and **200** via the intermediate **201**.

The chemical shifts of the methylene groups at C-3 and at C-5 at 52.0 ppm and 54.2 ppm, in the ^{13}C NMR spectrum of **199** indicated that the two methylenes were connected to a nitrogen atom, consistent with formation of an indolizidine structure. In castanospermine these methylene groups have similar ^{13}C NMR chemical shift at 51.9 and 55.7, respectively. In fact, all the indolizidine ring ^{13}C chemical shifts of **199** matched closely with that of castanospermine (compare Figure 23 with Figure 29). The C-5' and C-5 chemical shifts at 72.0 and 44.7 ppm, respectively, in the ^{13}C NMR spectrum of the compound **196** indicated that C-5' was connected to an oxygen atom and that C-5 was connected to nitrogen atom. The C-5 and C-2 chemical shift at 72.2

and 44.9 ppm, respectively, in the ^{13}C NMR spectrum of the compound **200** indicated that C-5 was connected to an oxygen atom and that C-2 was connected to nitrogen atom (Scheme 35). Due to the similar ^{13}C NMR chemical shifts of the side products **196** and **200** and also their same molecular weights, m/z = 370 ($M+H^+$, 100%) a HMBC (2 and 3-bonds correlation) experiment was used to characterize the structure of the compound **196**. The HMBC correlations of the compound **196** are shown in the Figure 21. The 3-bond correlation between C-2' and H-5' distinguished structure **196** over structure **200**. The latter compound would not be expected to show such as correlation between analogous carbon (C-8) and proton (H-5) in **200** as this would represent a 5-bond correlation.

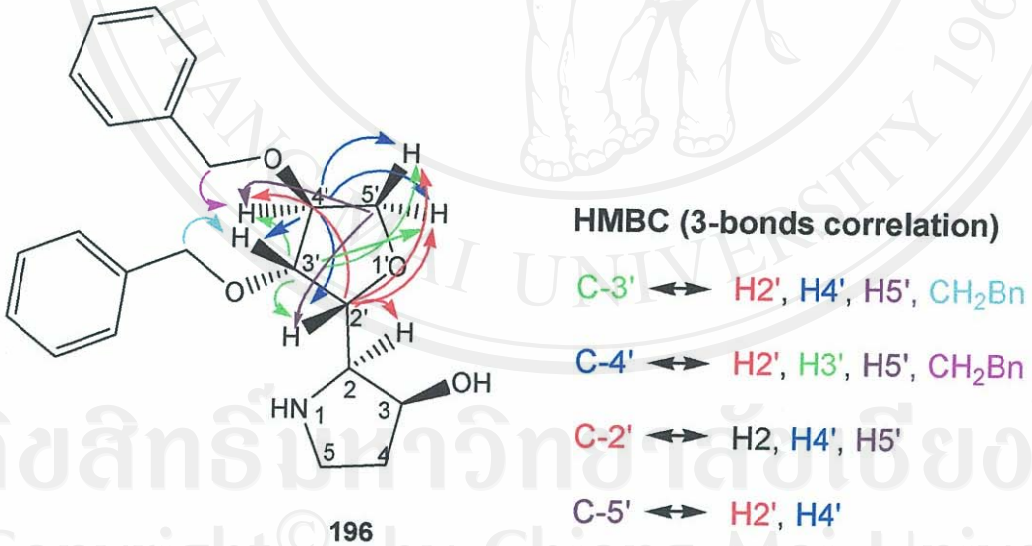

Figure 21 HMBC correlations of the compound **196**

The ^1H NMR and ^{13}C NMR spectra for compound **199**, were shown in Figures 22 and 23, respectively.

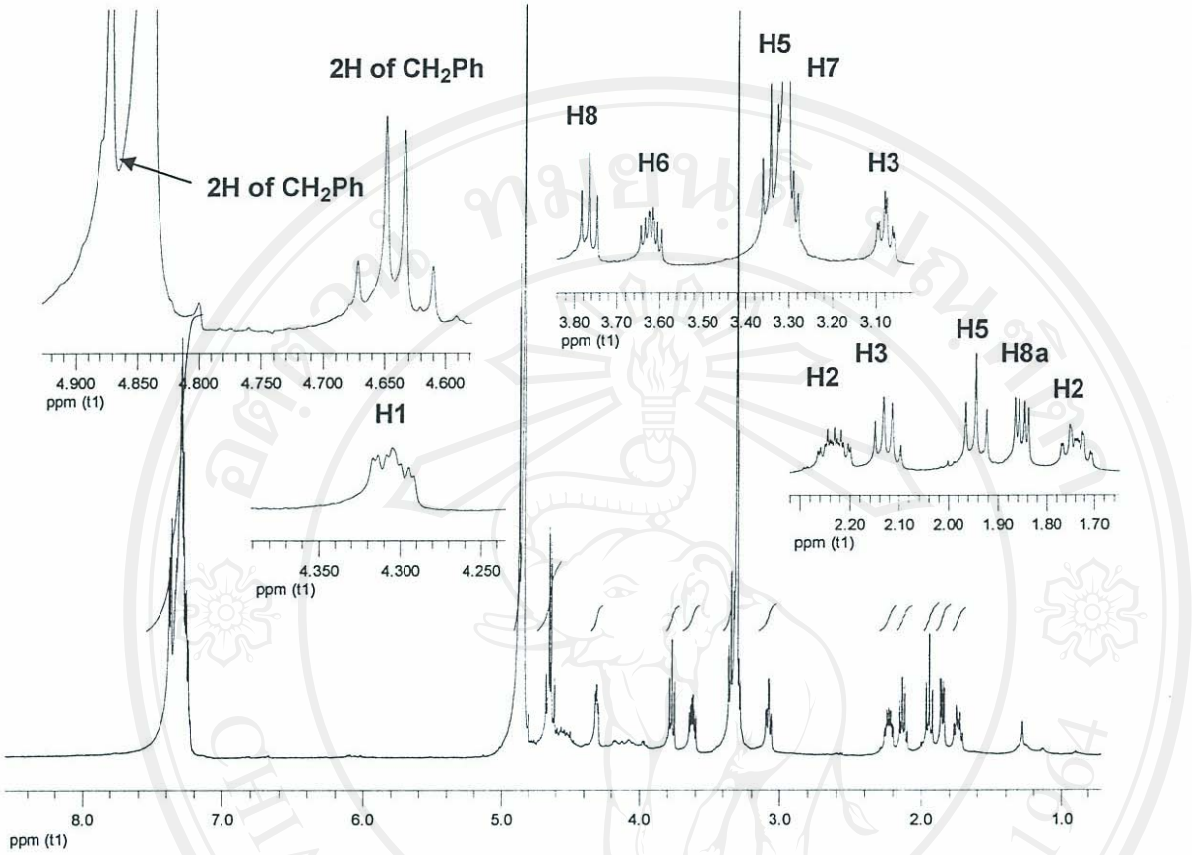

Figure 22 ^{1}H NMR spectrum (500 MHz, CD_3OD) of compound **199**

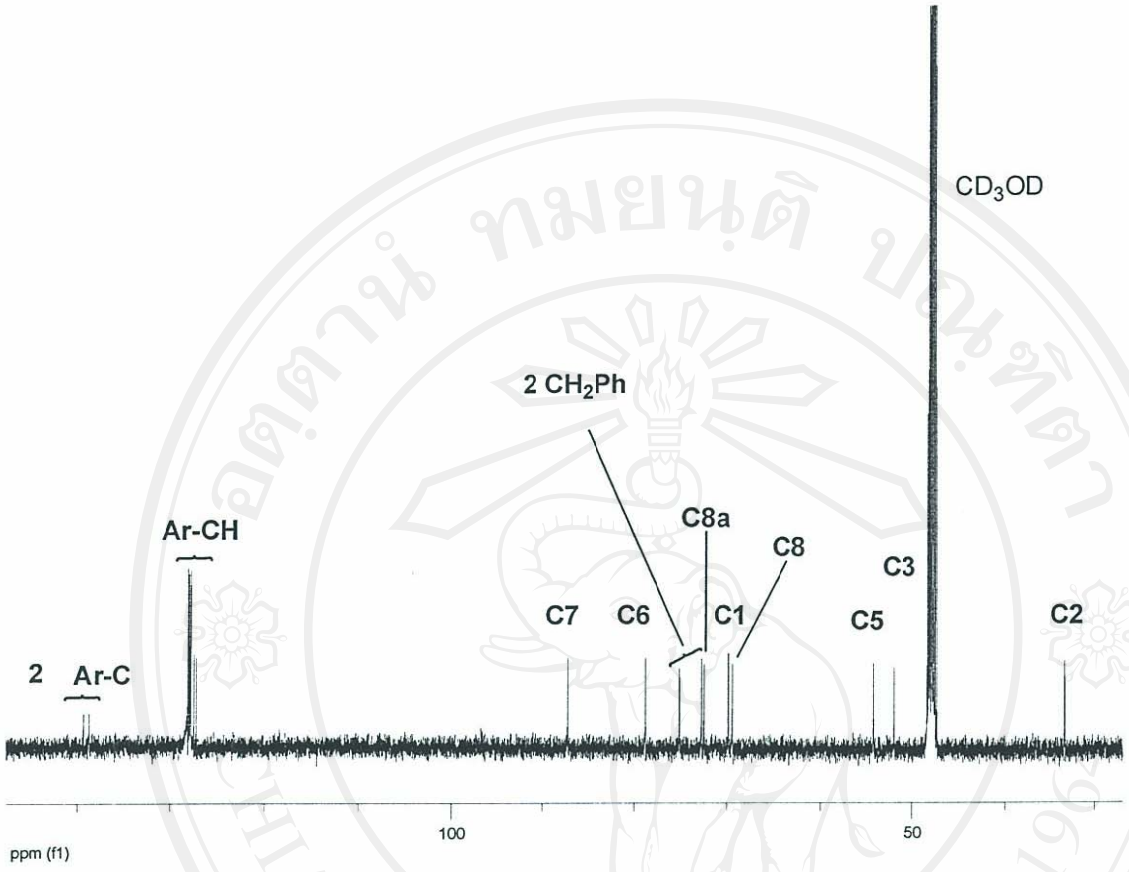

Figure 23 ^{13}C NMR spectrum (500 MHz, CD_3OD) of compound **199**

Finally, debenzylation of **199** by hydrogenolysis over $PdCl_2$ in methanol solution under an atmosphere of H_2 for 1 h at room temperature gave (+)-castanospermine **1a** in an excellent yield (95%) after purification by basic ion chromatography (Scheme 36).

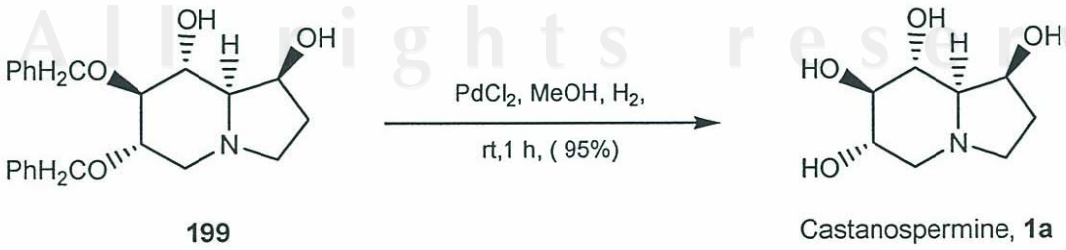

199 Castanospermine, **1a**

Scheme 36

The ^{1}H NMR (Figure 25) and ^{13}C NMR (Figure 28) spectra of synthetic (+)-castanospermine **1a** matched those reported in the literature [130], and an authentic sample of castanospermine (from Phytex) these data are shown in Table 7.

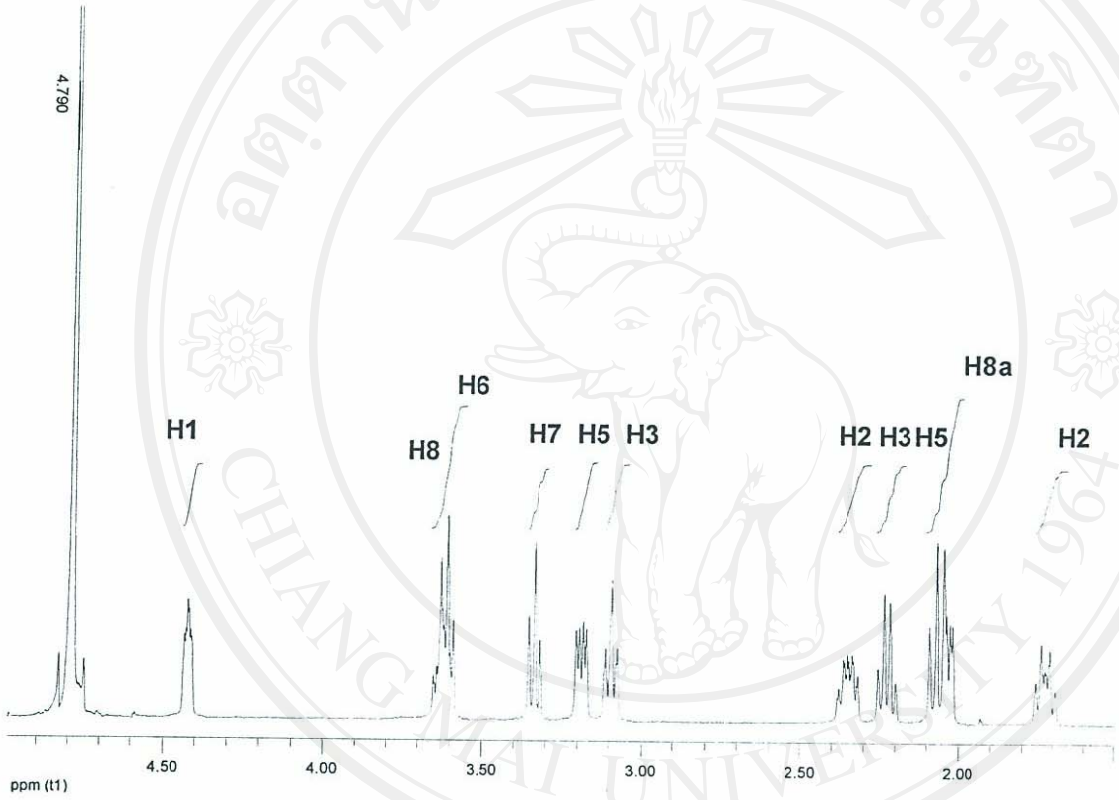

Figure 24 ^{1}H NMR spectrum (500 MHz, D_2O) of authetic (+)-castanospermine from Phytex, Australia

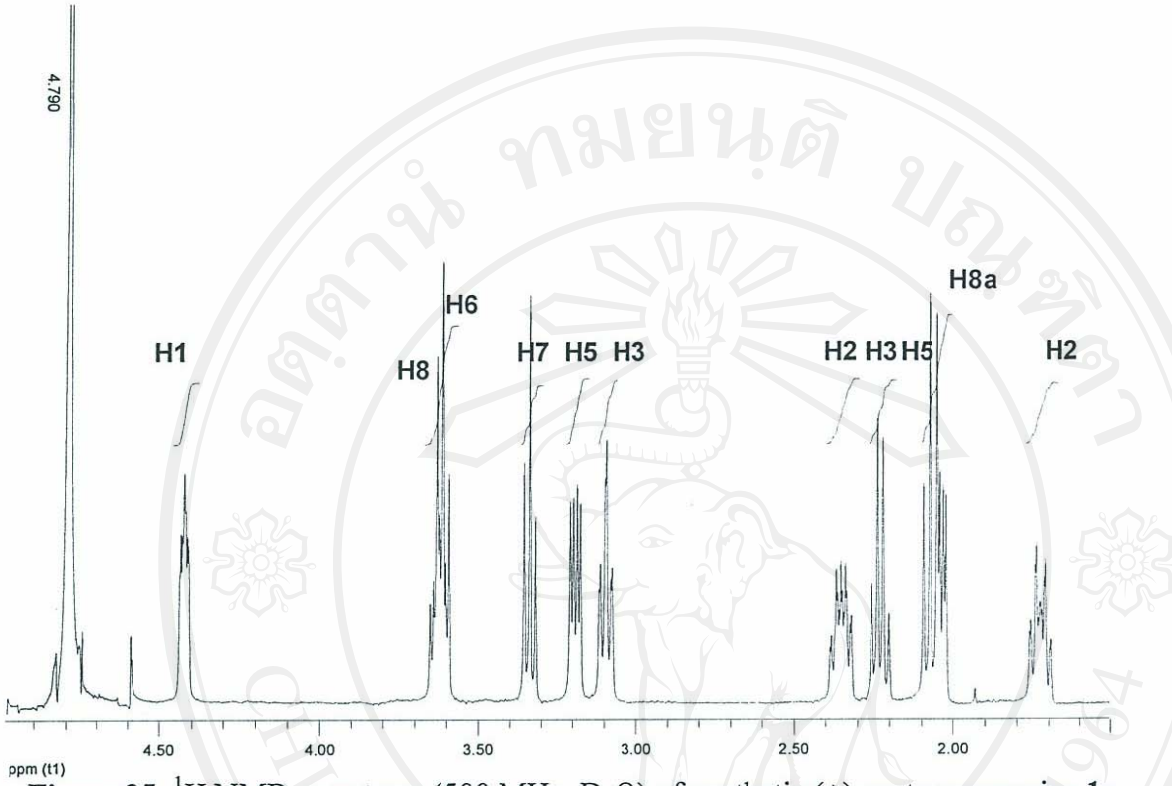

Figure 25 ^{1}H NMR spectrum (500 MHz, D_2O) of synthetic (+)-castanospermine **1a**

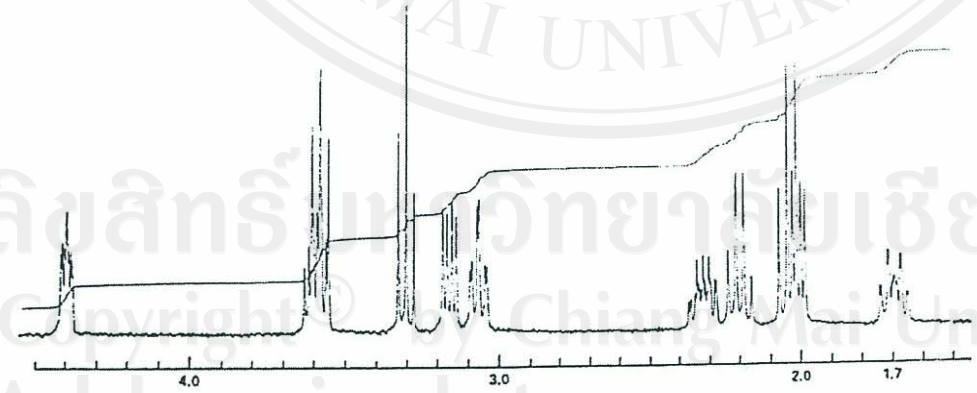

Figure 26 ^{1}H NMR spectrum (300 MHz, D_2O) of (+)-castanospermine, which was published in the journal *Phytochemistry* by Hohenschutz *et al.* (1981) [130].

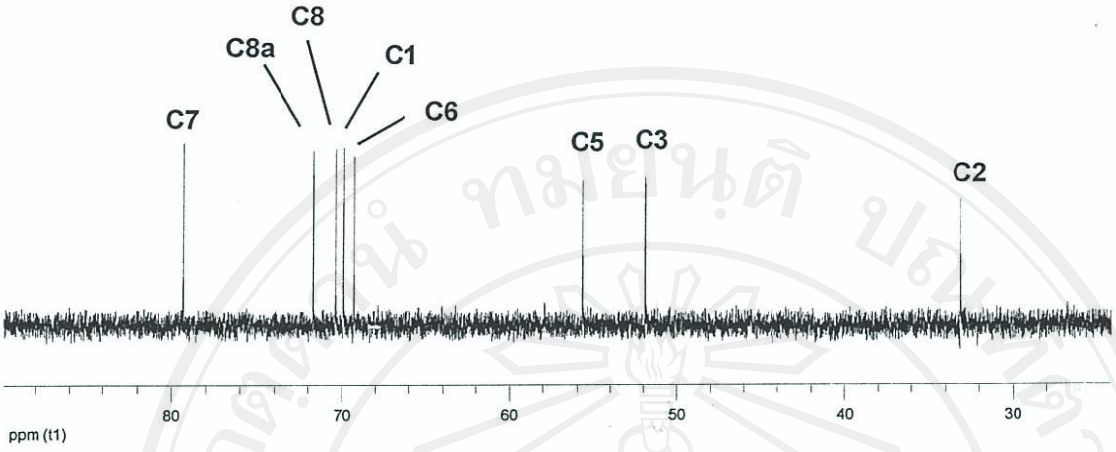

Figure 27 ^{13}C NMR spectrum (125 MHz, D_2O) of authentic (+)-castanospermine from Phytex, Australia

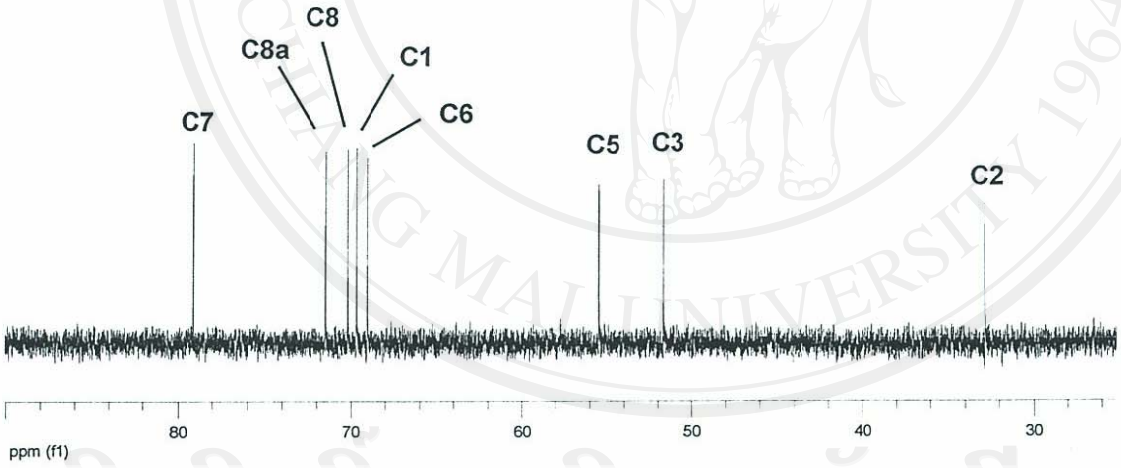

Figure 28 ^{13}C NMR spectrum (125 MHz, D_2O) of synthetic (+)-castanospermine **1a**

Table 7 Physical and ^{1}H NMR spectral data for the natural (+)-castanospermine, the synthetic (+)-castanospermine (**1a**) and the authentic (+)-castanospermine (Phytex)

	Natural (+)-Castanospermine [Ref. 130]	**Synthetic (+)-Castanospermine (1a)**	**Authentic (+)-Castanospermine** (From Phytex)
Physical appearance	Colorless microcrystal	Colorless crystal	Colorless crystal
Optical rotation	$[\alpha]_D^{24}$ + 79.7 (*c* 0.93, H_2O)	$[\alpha]_D^{27}$ + 82 (*c* 1.2, H_2O)	$[\alpha]_D^{28}$ + 83 (*c* 1.1, H_2O)
Meting point	212-215 °C	206-208 °C	213-215 °C
Mass spectrometry	*m/z* 189 (M^+)	ES+ *m/z* 190 ($M+H^+$, 100%)	ES+ *m/z* 190 ($M+H^+$, 100%)
^{1}H NMR	360 MHz, D_2O (HOD ref. at 4.8 ppm)	500 MHz, D_2O (HOD ref. at 4.79 ppm)	500 MHz, D_2O (HOD ref. at 4.79 ppm)
	1.70 (1H, dddd, $J_{2\beta,2\alpha}$ = 14, $J_{2\beta,3\alpha}$ = 10, $J_{2\beta,3\beta}$ = 10, $J_{2\beta,1}$ = 4.4, H2β)	1.72 (1H, dddd, $J_{2\beta,2\alpha}$ = 14, $J_{2\beta,3\alpha}$ = 8.5, $J_{2\beta,3\beta}$ = 8.5, $J_{2\beta,1}$ = 1.8, H2β)	1.72 (1H, dddd, $J_{2\beta,2\alpha}$ = 14, $J_{2\beta,3\alpha}$ = 8, $J_{2\beta,3\beta}$ = 8, $J_{2\beta,1}$ = 1.8, H2β)
	2.01 (1H, dd, $J_{8a,8}$ = 10, $J_{8a,1}$ = 4.4, H8a)	2.03 (1H, dd, $J_{8a,8}$ = 10, $J_{8a,1}$ = 4.5, H8a)	2.03 (1H, dd, $J_{8a,8}$ = 10, $J_{8a,1}$ = 4, H8a)
	2.04 (1H, dd, $J_{5\beta,5\alpha}$ = 10.7, $J_{5\beta,6}$ = 10, H5β)	2.07 (1H, t, $J_{5\beta,5\alpha}$ = $J_{5\beta,6}$ = 10.5, H5β)	2.07 (1H, t, $J_{5\beta,5\alpha}$ = $J_{5\beta,6}$ = 10, H5β)
	2.20 (1H, q, $J_{3\beta,2\beta}$ = $J_{3\beta,3\alpha}$ = $J_{3\beta,2\alpha}$ = 10, H3β)	2.23 (1H, q, $J_{3\beta,2\beta}$ = $J_{3\beta,3\alpha}$ = $J_{3\beta,2\alpha}$ = 9.5, H3β)	2.22 (1H, q, $J_{3\beta,2\beta}$ = $J_{3\beta,3\alpha}$ = $J_{3\beta,2\alpha}$ = 9, H3β)
	2.33 (1H, dddd, $J_{2\beta,2\alpha}$ = 14, $J_{2\alpha,3\beta}$ = 10, $J_{2\alpha,1}$ = 7, $J_{2\alpha,3\alpha}$ = 2, H2α)	2.35 (1H, dddd, $J_{2\beta,2\alpha}$ = 14, $J_{2\alpha,3\beta}$ = 9.5, $J_{2\alpha,1}$ = 7.5, $J_{2\alpha,3\alpha}$ = 2.5, H2α)	2.35 (1H, dddd, $J_{2\beta,2\alpha}$ = 14, $J_{2\alpha,3\beta}$ = 9, $J_{2\alpha,1}$ = 7, $J_{2\alpha,3\alpha}$ = 2, H2α)
	3.06 (1H, ddd, $J_{3\alpha,3\beta}$ = $J_{3\alpha,2\beta}$ = 10, $J_{3\alpha,2\alpha}$ = 2, H3α)	3.09 (1H, ddd, $J_{3\alpha,3\beta}$ = $J_{3\alpha,2\beta}$ = 9, $J_{3\alpha,2\alpha}$ = 2.5, H3α)	3.09 (1H, ddd, $J_{3\alpha,3\beta}$ = $J_{3\alpha,2\beta}$ = 9, $J_{3\alpha,2\alpha}$ = 2, H3α)
	3.16 (1H, dd, $J_{5\alpha,5\beta}$ = 10.7, $J_{5\alpha,6}$ = 5, H5α)	3.19 (1H, dd, $J_{5\alpha,5\beta}$ = 10.5, $J_{5\alpha,6}$ = 5, H5α)	3.19 (1H, dd, $J_{5\alpha,5\beta}$ = 10, $J_{5\alpha,6}$ = 5, H5α)
	3.30 (1H, t, $J_{7,8}$ = $J_{6,7}$ = 8.5, H7)	3.34 (1H, t, $J_{7,8}$ = $J_{6,7}$ = 9.5, H7)	3.33 (1H, t, $J_{7,8}$ = $J_{6,7}$ = 9, H7)
	3.58 (1H, dd, $J_{8,8a}$ = 10, $J_{8,7}$ = 8.5, H8)	3.61 (1H, t $J_{8,8a}$ = $J_{8,7}$ = 9.5, H8)	3.61 (1H, t $J_{8,8a}$ = $J_{8,7}$ = 9, H8)
	3.60 (1H, ddd, $J_{6,5\beta}$ = 10, $J_{6,7}$ = 8.5, $J_{6,5\alpha}$ = 5, H6)	3.63 (1H, ddd, $J_{6,5\beta}$ = 10.5, $J_{6,7}$ = 9.5, $J_{6,5\alpha}$ = 5, H6)	3.64 (1H, ddd, $J_{6,5\beta}$ = 10, $J_{6,7}$ = 9, $J_{6,5\alpha}$ = 5, H6)
	4.40 (1H, ddd, $J_{1,2\alpha}$ = 7, $J_{1,8a}$ = 4.4, $J_{1,2\beta}$ = 2, H1)	4.42 (1H, ddd, $J_{1,2\alpha}$ = 7, $J_{1,8a}$ = 4.5, $J_{1,2\beta}$ = 1.8, H1)	4.42 (1H, ddd, $J_{1,2\alpha}$ = 7, $J_{1,8a}$ = 4, $J_{1,2\beta}$ = 1.8, H1)

Table 8 ^{13}C NMR spectral data for natural (+)-castanospermine, the synthetic (+)-castanospermine **1a** and an authentic sample of (+)-castanospermine (Phytex)

	Natural (+)-Castanospermine [Ref. 130]	**Synthetic (+)-Castanospermine (1a)**	**Authentic (+)-Castanospermine** (Phytex)
^{13}C NMR	22.5 MHz, D_2O, Dioxan Ref. (δ = 66.5 ppm)	125 MHz, D_2O (Acetone Ref. at 30.89 ppm)	125 MHz, D_2O (Acetone Ref. at 30.89 ppm)
	79.0 (CH, C7)	79.3 (CH, C7)	79.3 (CH, C7)
	71.2 (CH, C8a)	71.7 (CH, C8a)	71.7 (CH, C8a)
	70.4 (CH, C8)	70.4 (CH, C8)	70.4 (CH, C8)
	69.4 (CH, C1)	69.9 (CH, C1)	69.9 (CH, C1)
	69.2 (CH, C6)	69.2 (CH, C6)	69.3 (CH, C6)
	55.4 (CH_2, C5)	55.7 (CH_2, C5)	55.7 (CH_2, C5)
	51.6 (CH_2, C3)	51.8 (CH_2, C3)	51.9 (CH_2, C3)
	33.1 (CH_2, C2)	33.0 (CH_2, C2)	33.0 (CH_2, C2)

In summary, we have developed a diastereoselective synthesis of the indolizidine alkaloid castanospermine **1a** by using the Petasis reaction as the first step to condense the three components, L-xylose, allylamine and *trans*-phenylboronic acid. A RCM reaction was employed to form the pyrrolo[1,2-*c*]oxazol-3-one precursor **189**. *Syn*-dihydroxylation of **189** was performed as the key step for construction of **194** which had the stereochemistry of the C-7 hydroxy group the same as the C-3 hydroxy of castanospermine **1a**. After base hydrolysis of oxazolidinone ring of **194**, the resulting product **195** was cyclized to form the indolizidine ring **199** using the Mitsunobu reaction. The desired product **1a** was obtained in an excellent yield after the debenzylation of **199**.